



SimuLAMP™

Software for Optical and Thermal Design and
Optimization of LED Lamps and Arrays

Physics Summary

Version 2.0

April, 2012



STR IP Holding, LLC, Richmond, VA, USA
Copyright © 2010-2012 by STR IP Holding, LLC.
All rights reserved. Published 2012.

This manual is the confidential and proprietary product of STR IP Holding, LLC. Any unauthorized use, reproduction, or disclosure of this manual is strictly prohibited. (Subject to limited use within the STR End-User License Agreement only.)

CGSim™, VR™, PolySim™, CVDSim™, HEpiGaNS™, SimuLED™, SiLENSe™, RATRO™, SpeCLED™, SimuLAMP™, SELES™, FETIS™ are registered trademarks, brands, and proprietary products of STR IP Holding, LLC.

User Support: SimuLED-support@str-soft.com
Software Sales: STR-sales@str-soft.com
Phone: +7 812 320 4390 Fax: +7 812 326 6194
STR Group Ltd. www.str-soft.com
Engels av. 27, P.O. Box 89, 194156, St. Petersburg, Russia

Table of Contents

1	Introduction.....	4
2	Ray tracing procedure	5
3	The model of light conversion and ray tracing in the conversion medium.....	6
3.1	Input characteristics.....	6
3.2	Calculated characteristics.....	7
3.3	Scattering models.....	7
3.3.1	Mie model of scattering.....	8
3.3.2	Rayleigh model of scattering.....	8
3.3.3	Henney-Greenstein model of scattering	9
3.4	Light propagation in the conversion medium	9
4	Computation of the color coordinates and rendering Index	11
4.1	Color coordinates.....	11
4.2	Correlated color temperature	12
4.3	Color rendering index	13
4.4	Integral characteristics.....	14
5	Computation of power and luminous characteristics of LED lamp.....	15
6	Heat transfer and heat sources in the lamp	17
6.1	Heat transfer.....	17
6.2	Heat sources in the lamp.....	17
6.2.1	Self-heating of LED chips	17
6.2.2	Heat release in conversion medium.....	18
6.2.3	Light absorption in the lamp units and boundaries.....	18
7	References	20



1 Introduction

SimuLAMP software package is intended for modeling operation of LED lamps. The software simulates light propagation inside an LED lamp by ray tracing with account of light scattering at all optical boundaries. It allows computation of the luminous and color characteristics of light emitted by the lamp (luminous efficiency, emission spectrum, color rendering index, correlated color temperature, etc.) and angular distributions of the characteristics in the far field. The simulator solves also the heat transfer problem and predicts the temperature distribution inside the LED lamp, which can be used for optimization of the lamp design. It is possible to get coupled solution of the optical and thermal problems in a package of complex design, accounting for heat release in both the LED chip due to its self-heating and conversion medium due to the light absorption by phosphor particles and Stokes shift related to the light conversion. **SimuLAMP** allows simulations of white-light LED lamps with conversion medium containing either a single phosphor or phosphor mixture. Advanced models of light conversion based on the Mie theory are used for the simulations. The package supports the lamp designs with single- or multichip package configurations including RGB LEDs and multi-pixel LED arrays. It enables the analysis of the lamp operation in DC/AC/Quasi-CW modes.

This document describes the basic physical models implemented in the **SimuLAMP** package.

2 Ray tracing procedure

Spectral ray tracing procedure simulates propagation of photons inside the LED lamp and their extraction from the lamp. Photons are assumed to be emitted from the surface of the LED chip with either isotropic or Lambertian emission pattern. The wavelength of a photon is determined via random choice with the probability corresponding to the LED emission spectrum. The same approach is used to obtain the initial direction of the photon propagation according to the emission pattern specified by user. The initial energy of the photon W_{ph} is assumed to be equal the ratio of the LED chip optical power to the number of traced rays specified by the user, and it decreases along the photon pathway as

$$W_{ph} = W_{ph}^0 \exp(-\alpha_i L), \quad (2.1)$$

where α_i is the absorption coefficient in the material and L is the path passed by the photon.

The photon may either change its propagation direction or be absorbed at optical boundaries (boundaries between the media with different refractive indexes) and by phosphor particles embedded in a conversion medium. Three types of the optical boundaries are distinguished in the package: smooth, mirror-like, and LED ones.

The photon reflection/transmission at the smooth boundary obeys the Fresnel's law [1]. The reflection R and transmission T coefficients are considered as the probabilities of photon reflection and refraction, respectively, so the photon can either go to another medium (with probability T) or be reflected and then propagate in the same medium (with probability R). The direction of the photon reflection or refraction follows the Snell's law [1].

When the photon reaches the mirror-like boundary, various physical processes may occur. The photon may be reflected, transmitted, or scattered with the user-defined probabilities. The scattering is assumed to be diffusive, so that the direction of scattering is chosen following the Lambert's law.

The LED boundary type is assigned for the boundary separating submount and LED chip. Approaching that boundary, the photon is assumed to be absorbed.

The photon propagates inside the lamp until it either leaves it or its intensity I becomes less than the critical value specified by user. After that the photon tracing is finished and the tracing of the next one starts again. The procedure is repeated until the total number of traced photons exceeds the maximum number set by user.

3 The model of light conversion and ray tracing in the conversion medium

3.1 Input characteristics

Conversion medium is considered as a mixture of various phosphor particles embedded into an immersion medium, which are able to scatter, absorb, and then reemit light. An arbitrary number of the conversion media can be considered in the **SimuLAMP** package since the version 2.0.

The parameters and characteristics of every conversion medium are:

- spectral and temperature dependence of the immersion medium refractive index $n_m(\lambda, T)$
- number N and types of the phosphors embedded ($p = 1 \dots N$)
- particle density of the p -th phosphor N_p [cm^{-3}]
- experimental or user-defined distribution $G(r_p)$ of the p -th phosphor particle sizes (radii r_p)
- experimental or approximated temperature-dependent excitation spectrum $E_p(\lambda, T)$ of the p -th phosphor specified in relative units
- experimental or approximated temperature-dependent emission spectrum $L_p(\lambda, T)$ of the p -th phosphor specified in relative units
- spectral and temperature dependence of the real part of the refractive index $n'_p(\lambda, T)$ of the p -th phosphor (this dependence must be defined in the spectral range covering the emission and excitation spectra of all the phosphors and LEDs used in the lamp)
- absorption coefficient of the p -th phosphor $\alpha_p(\lambda_p, T_p)$ [cm^{-1}] at a certain wavelength λ_p measured at temperature T_p
- temperature-dependent quantum efficiency $\eta_p(T)$ of light emission by the p -th phosphor, approximated by the expression

$$\eta_p(T) = \frac{\eta_0}{1 + \exp\left(\frac{T - T_1}{T_2}\right)}, \quad (3.1)$$

where T_1 and T_2 – parameters with the meaning of temperatures specified by user.

3.2 Calculated characteristics

The following characteristics are calculated from the input ones before modeling the light conversion:

- wavelength dependence of the absorption coefficient of the p -th phosphor material

$$\alpha_p(\lambda) = \alpha_p(\lambda_p, T_p) \cdot E_p(\lambda, T) / E_p(\lambda_p, T_p) \quad (3.2)$$

Here T is the reference temperature equal, for instance, the mean temperature of the conversion medium in the LED lamp.

- spectral and temperature dependence of the imaginary part of the particle refractive index of the p -th phosphor

$$n_p''(\lambda) = \lambda \alpha_p(\lambda) / 4\pi \quad (3.3)$$

- spectral dependence of the extinction $\sigma_{\text{ext}}^{(p)}(\lambda)$, scattering $\sigma_{\text{sct}}^{(p)}(\lambda)$ and absorption $\sigma_{\text{abs}}^{(p)}(\lambda)$ cross-sections of the phosphor particles computed within a chosen light scattering model with account of the experimental particle size distribution $G(r_p)$; these cross-sections are related with each other by the equation

$$\sigma_{\text{ext}}^{(p)}(\lambda) = \sigma_{\text{sct}}^{(p)}(\lambda) + \sigma_{\text{abs}}^{(p)}(\lambda) \quad (3.4)$$

- light scattering pattern $F_p(\tau, \lambda)$ averaged by the light polarizations (see Sec.3.3), where $\tau = \cos \theta$, and θ is the polar angle of scattering (the angle between the propagation directions of incident and scattered photons); this pattern is calculated with account of the experimental particle size distribution $G(r_p)$
- asymmetry factor $g_p(\lambda)$ being the first moment of the Mie scattering pattern, which can be used in the Henney-Greenstein empirical model of light scattering (see Sec.3.3.3); this factor is calculated with account of the experimental particle size distribution $G(r_p)$

3.3 Scattering models

There are three scattering models that can be used for calculations of scattering/absorption cross-sections and scattering pattern in **SimuLAMP** simulator. The Mie model considers the light interaction with the spherical particles of arbitrary size. The Rayleigh model is applicable to nano-phosphors with the particle sizes much less than the wavelength of light. The Henney-Greenstein model is based on

the empirical formula for the scattering pattern, which is found to work well as the approximation for various experimental data on the light scattering by particles, dust, aerosols, etc.

3.3.1 Mie model of scattering

The Mie model characterizes light scattering by absorbing spherical particles of an arbitrary size [2]. The extinction, scattering, and absorption cross-sections are calculated numerically as a function of the light wavelength and the particle radius. After averaging over the particle sizes with the distribution function $G(r_p)$ the cross-sections become dependent on the wavelength only.

The scattering pattern is calculated numerically for a number of wavelengths within a given spectral range with averaging then over the particle sizes. To obtain the pattern for a desirable wavelength, an interpolation procedure is applied.

3.3.2 Rayleigh model of scattering

Rayleigh model is used for characterization of light scattering by spherical particles of the small size (much less than the scattering light wavelength value). The analytical expressions borrowed from [3] are used to calculate the extinction, scattering, and absorption cross-sections. Within this model, the scattering pattern is independent neither of the light wavelength nor of the particle size and can be obtained analytically as

$$F_p(\tau, \lambda) = \frac{3}{8}(1 + \tau^2) \quad , \quad \tau = \cos \theta \quad (3.5)$$

The Rayleigh approach is normally applied to nano-phosphor conversion media with relatively high concentrations of the phosphor particles. In this case, the mean distance between the particles is much less than the wavelength of light. This modifies the refractive index of the conversion medium as a whole. To calculate the effective refractive index n or dielectric constant ε , two approaches are used:

- The Bruggeman model [4]

$$\varepsilon(\lambda) = \varepsilon_* + \sqrt{\varepsilon_*^2 + \varepsilon_m \varepsilon_p} / 2 \quad , \quad \varepsilon_* = \frac{\varphi_m(2\varepsilon_m - \varepsilon_p) + \varphi_p(2\varepsilon_p - \varepsilon_m)}{4} \quad (3.6)$$

- The Monecke model [5]

$$\varepsilon(\lambda) = \frac{2(\varphi_m \varepsilon_m + \varphi_p \varepsilon_p)^2 + \varepsilon_m \varepsilon_p}{(1 + \varphi_m) \varepsilon_m + (1 + \varphi_p) \varepsilon_p} \quad \rightarrow \quad n(\lambda) = \varepsilon^{1/2}(\lambda) \quad , \quad (3.7)$$

where $\varepsilon_m = n_m^2$, $\varepsilon_p = (n'_p)^2$, $\varphi_m = 1 - \varphi_p$, and φ_p is the volume fraction of phosphor particles in the conversion medium.

The obtained refractive index spectral dependence affects the photon propagation in the conversion medium according to Fresnel's and Snell's laws, see Sec.3.4.

3.3.3 Henney-Greenstein model of scattering

The model by Henney-Greenstein deals with the scattering pattern, rather than with the extinction, scattering, and absorption cross-sections. The scattering pattern is approximated by the empirical formula having only one parameter – asymmetry factor $g_p = g_p(\lambda)$ [6]:

$$F_p^{HG}(\cos \theta, \lambda) = \frac{1 - g_p^2}{2(1 + g_p^2 - 2g_p \cos \theta)^{3/2}}, \quad (3.8)$$

This parameter can be either set manually by the user or obtained from the Mie theory (see Sec.3.2).

3.4 Light propagation in the conversion medium

The initial direction of photon propagation in the conversion medium is obtained from analysis of the photon reflection/refraction at the smooth optical boundary surrounding the conversion medium (see Sec.2). Then the photon starts to propagate inside the medium until it interacts with a phosphor particle.

Let a conversion medium to contain the mixture of phosphors ($p = 1 \dots N$). The total extinction length $l_{\text{tot}}(\lambda)$ of the photons in the conversion medium is defined by the expression

$$l_{\text{tot}}^{-1}(\lambda) = \sum_{p=1}^N N_p \sigma_{\text{ext}}^{(p)}(\lambda) \quad (3.9)$$

The probability of light interaction P_i (absorption or scattering by the phosphor particles) after passing the path L is calculated by the expression

$$P_i(\lambda) = 1 - \exp[-L/l_{\text{tot}}(\lambda)] \quad (3.10)$$

P_i can be obtained from the generation of the random number R within the $[0,1]$ interval; then the free photon path before the event of its interaction with the phosphor particle is found as:

$$L = -l_{\text{tot}}(\lambda) \cdot \ln(1 - R) .$$

If the value of L is larger than the possible path to the next boundary of the conversion medium, the photon is considered to reach that boundary without interacting with particles. Then the ray-tracing of the photon is continued in a way discussed in Sec.2. If the value of L is less than the possible path to the next boundary, an interaction with a particle is considered to occur.

The next step is to define the type of that particle with which the interaction takes place. The probability P_p of the photon interaction (scattering or absorption) just with the p -th phosphor particles is

$$P_p(\lambda) = l_{\text{tot}}(\lambda) N_p \sigma_{\text{ext}}^{(p)}(\lambda) \quad (3.11)$$

The type of interacting phosphor is determined by a random choice accounting for the above probabilities P_p .

Two types of physical processes may occur as a result of photon-particle interaction, which are either scattering or absorption. The probabilities of the light scattering P_p^{sct} and absorption P_p^{abs} by the p -th phosphor particles are calculated as

$$P_p^{\text{sct}}(\lambda) = \sigma_{\text{sct}}^{(p)} / \sigma_{\text{ext}}^{(p)} \quad , \quad P_p^{\text{abs}}(\lambda) = \sigma_{\text{abs}}^{(p)} / \sigma_{\text{ext}}^{(p)} \quad (3.12)$$

These probabilities are used to determine the type of the interaction event (scattering or absorption).

The wavelength of light is not changed upon scattering by the phosphor particles, but the scattered photons changes its propagation direction. The azimuthal angle of photon scattering is obtained by a random choice, assuming its isotropic in-plane distribution. The polar scattering angle is obtained numerically from the computed scattering pattern by considering the pattern as the distribution of the probability density for the photon scattering.

If the photon is absorbed by the p -th phosphor, it either reemits light with the probability $\eta_p(T)$ or transforms its energy to heat via non-radiative recombination with the probability $1 - \eta_p(T)$. Here, $\eta_p(T)$ is the quantum efficiency of light emission by the p -th phosphor. Reemitted photon has a different wavelength, which is determined from the phosphor emission spectrum, considering it as the distribution of the spectral probability density. The propagation direction of the reemitted photon is assumed to be random (the reemission pattern is considered to be isotropic).

4 Computation of the color coordinates and rendering index

Photons with different wavelength extracted from the LED lamp are counted in the far-field zone to produce the emission spectra $S(\lambda)$ corresponding to a certain observation angle. These spectra are analyzed to estimate the white light quality in terms of conventional characteristics.

The emission spectrum $S(\lambda)$ can be characterized by the following parameters:

- color coordinates x and y in the CIE color diagram
- correlated color temperature (CCT)
- color rendering index (CRI)

4.1 Color coordinates

The color coordinates in the CIE 1931 XYZ color space are found from the standard color matching functions $\bar{x}(\lambda)$, $\bar{y}(\lambda)$, and $\bar{z}(\lambda)$, which are presented in **Fig.1**.

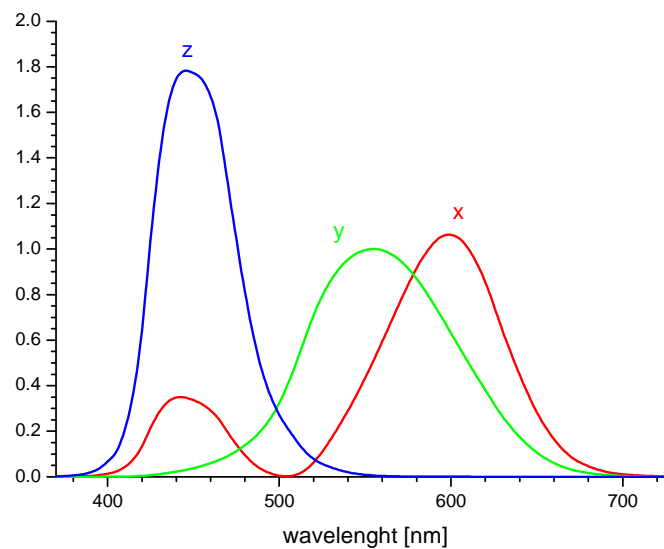


Fig.1. Spectral dependence of the standard color matching functions

The tristimulus values X , Y and Z are defined as follows

$$X = k \int S(\lambda) \cdot \bar{x}(\lambda) \cdot d\lambda \quad (4.1)$$

$$Y = k \int S(\lambda) \cdot \bar{y}(\lambda) \cdot d\lambda \quad (4.2)$$

$$Z = k \int S(\lambda) \cdot \bar{z}(\lambda) \cdot d\lambda \quad (4.3)$$

Here $k = \frac{100}{\int S(\lambda) \cdot \bar{y}(\lambda) \cdot d\lambda}$, so that Y is normalized to the value of 100.

Then the derived color coordinates x and y are found from the tristimulus values by normalizing to unity as

$$x = \frac{X}{X + Y + Z} \quad (4.4)$$

$$y = \frac{Y}{X + Y + Z} \quad (4.5)$$

4.2 Correlated color temperature

The CCT value is found using Robertson's method as follows. First, the (u, v) space color coordinates are found from the known (x, y) ones by using the relationships

$$u = \frac{4x}{-2x + 12y + 3} \quad (4.6)$$

$$v = \frac{6y}{-2x + 12y + 3} \quad (4.7)$$

Then two nearest isotherms with known color temperatures T_1 and T_2 are identified on the (u, v) chromaticity diagram. The CCT value T_c is found as

$$T_c = T_1 + \frac{d_1}{d_1 - d_2} (T_2 - T_1) \quad (4.8)$$

where d_1 and d_2 are the distances from the (u, v) -point to the corresponding isotherms, which are defined as

$$d_i = \frac{(v - v_i) - t_i(u - u_i)}{\sqrt{1 + t_i^2}} \quad (4.9)$$

where (u_i, v_i) and t_i are the coordinates and the tangent of the slope of the i -th isotherm, respectively, which are tabulated in the temperature range from 1,000 to 30,000 K.

4.3 Color rendering index

The light source CRI is calculated with reference to a standard illuminant with the same value of CCT as that of the measured light source. The standard illuminant is characterized by a known emission spectrum $P(\lambda)$ and respective color coordinates (u_0, v_0) corresponding to this spectrum.

Then chromaticity of the standard test color samples with given reflection spectra $r_i(\lambda)$ is calculated for their illumination by both measured and standard illuminants as follows:

$$\begin{aligned} X_{S_i} &= k \int r_i(\lambda) \cdot S(\lambda) \cdot \bar{x}(\lambda) \cdot d\lambda \\ Y_{S_i} &= k \int r_i(\lambda) \cdot S(\lambda) \cdot \bar{y}(\lambda) \cdot d\lambda \\ Z_{S_i} &= k \int r_i(\lambda) \cdot S(\lambda) \cdot \bar{z}(\lambda) \cdot d\lambda \end{aligned} \quad (4.10)$$

$$\begin{aligned} X_{P_i} &= k \int r_i(\lambda) \cdot P(\lambda) \cdot \bar{x}(\lambda) \cdot d\lambda \\ Y_{P_i} &= k \int r_i(\lambda) \cdot P(\lambda) \cdot \bar{y}(\lambda) \cdot d\lambda \\ Z_{P_i} &= k \int r_i(\lambda) \cdot P(\lambda) \cdot \bar{z}(\lambda) \cdot d\lambda \end{aligned} \quad (4.11)$$

The tristimulus values are used to calculate first the coordinates in (u, v) -color space and then the coordinates in (W^*, U^*, V^*) -color space as

$$\begin{aligned} W^* &= 25 \cdot Y^{1/3} - 17 \\ U^* &= 13 \cdot W^* (u - u_0) \\ V^* &= 13 \cdot W^* (v - v_0) \end{aligned} \quad (4.12)$$

The color rendering indices for each test sample are found as

$$\begin{aligned} R_i &= 100 - 4.6 \Delta E_i \\ \Delta E_i &= \sqrt{(W_{P_i} - W_{S_i})^2 + (U_{P_i} - U_{S_i})^2 + (V_{P_i} - V_{S_i})^2} \end{aligned} \quad (4.13)$$

Finally, the total color rendering index is found as

$$R = \frac{1}{N} \sum_{i=1}^N R_i \quad (4.14)$$

Two sets of the standart test color samples, which are the 8 color and the 14 color sets [7], are used in the simulator, thus the two values of the CRI are calculated.

4.4 Integral characteristics

Along with the color characteristics corresponding to a certain observation angle, the integral characteristics are also computed in the **SimuLAMP** package by integrating the emission spectra of the lamp in the far-field zone.

5 Computation of power and luminous characteristics of LED lamp

Another group of characteristics computed by the package are power and luminous characteristics of the LED lamp, namely, the angular distributions of the radiant intensity and luminous flux of the light extracted from the lamp and luminous efficacy of radiation and source.

First, the energy of each “photon” emitted from the chip surface is calculated as a ratio of the total optical power provided by LED chip to the number of traced photons specified by user. The energies of the photons extracted from the LED lamp are counted in the far-field zone to produce the radiant intensity $P_{\theta,\varphi}$ corresponding to a certain observation angle θ . The angular distribution of the radiant intensity integrated over the azimuthal angles φ determines the radiant pattern P_{θ} , being given in the solver result tab. By integrating the radiant intensity distribution in the far-field zone over the observation angle θ , the total optical power P_{tot} of the lamp is computed.

The luminous flux Φ_{θ} distribution of the extracted light is obtained as follows

$$\Phi_{\theta} = P_{\theta} \cdot LE_0 \cdot \int_0^{\infty} S_{\theta}(\lambda)V(\lambda)d\lambda, \quad (5.1)$$

where $S_{\theta}(\lambda)$ is the emission spectra corresponding to a certain observation angle θ , $V(\lambda)$ is the standard luminosity function (spectral eye response) and $LE_0 = 683 \frac{lm}{W}$ is the luminous efficacy of an ideal monochromatic 555 nm light source.

The total luminous flux Φ_{tot} is derived from the total optical power as

$$\Phi_{tot} = P_{tot} \cdot LE_0 \cdot \int_0^{\infty} S(\lambda)V(\lambda)d\lambda, \quad (5.2)$$

where $S(\lambda)$ corresponds to the emission spectrum of the lamp integrated over the observation angles.

Using the total optical power and luminous flux we further compute the luminous efficacy of radiation:

$$LE_{rad} = \frac{\Phi_{tot}}{P_{tot}} \quad (5.3)$$



The luminous efficacy of the source is computed by replacing P_{tot} in Eq.(5.3) with the input electrical power P_{in} :

$$LE_{source} = \frac{\Phi_{tot}}{P_{in}} \quad (5.4)$$

6 Heat transfer and heat sources in the lamp

6.1 Heat transfer

To obtain the temperature distribution inside the lamp, the heat transfer equation is solved:

$$c(\mathbf{r},T)\rho(\mathbf{r},T)\frac{\partial T}{\partial t} = \nabla \cdot [\kappa(\mathbf{r},T)\nabla T] + Q(\mathbf{r},T) \quad , \quad (6.1)$$

where T is temperature at the point with the radius-vector \mathbf{r} and time t , $c(\mathbf{r},T)$ and $\rho(\mathbf{r},T)$ are the specific heat capacity and density of the material, respectively, $\kappa(\mathbf{r},T)$ is the heat conductivity of the material, and $Q(\mathbf{r},T)$ is the heat source power density.

The general boundary conditions used for Eq.(6.1) are

$$-\kappa(\mathbf{n} \cdot \nabla T_S) = \alpha(T_S - T_a) + \varepsilon\sigma(T_S^4 - T_a^4) \quad , \quad (6.2)$$

where ∇T_S and T_S are the temperature gradient and temperature at the boundary surface, T_a is the ambient temperature, \mathbf{n} is the normal to the surface, α is the heat transfer coefficient, ε is the emissivity coefficient, and σ is the Stefan-Boltzmann constant. At $\varepsilon = 0$, the boundary conditions describe the heat release from the surface corresponding to the thermal resistance $R_{th} = A/\alpha$ (A is the area of the surface through which the heat is released). At $\alpha = 0$, the heat is removed from the surface via radiation.

6.2 Heat sources in the lamp

There are three types of the heat source in the lamp, namely, self-heating of the LED chips, light absorption and Stokes shift release in the conversion medium, and light absorption in the lamp units and boundaries. Let us consider each type in more detail.

6.2.1 Self-heating of LED chips

The power density of the current- and temperature-dependent heat release in an LED chip $Q_{LED}(I,T)$ can be calculated as

$$Q_{LED}(I,T) = P_{in}(I,T)[1 - WPE(I,T)] \quad , \quad (6.3)$$

where $P_{in}(I, T) = I \cdot V(I, T)$ is the electrical power supplied to the LED and derived from the temperature-dependent current-voltage characteristic, and $WPE(I, T)$ is the wall-plug efficiency of the LED chip. This heat release is taken into account in the heat transfer analysis via the boundary condition on the surface of the chip, written as follows

$$-\kappa(\mathbf{n} \cdot \nabla T_s) = q_s \quad , \quad (6.4)$$

where q_s is the heat flux outgoing from the chip surface of the area A , defined as $q_s = \frac{Q_{LED}}{A}$.

6.2.2 Heat release in the conversion medium

Here the heat release originates from the light absorption by the phosphor particles. In the case of the absorption without light conversion, the total energy of the incident photon W_{ph} is transformed into the heat. In the case of absorption followed by light conversion, the energy of the reemitted photon \tilde{W}_{ph} is reduced due to the Stokes shift:

$$\tilde{W}_{ph} = W_{ph} \cdot \frac{\lambda}{\tilde{\lambda}} \quad , \quad (6.5)$$

where $\tilde{\lambda}$ is the wavelength of the reemitted photon. The difference in energies of the incident and reemitted photons is converted into the heat

$$W_{Stokes} = W_{ph} \cdot \left(1 - \frac{\lambda}{\tilde{\lambda}}\right) \quad (6.6)$$

The heat release is considered to take place inside the grid cell in which the interaction of light with the phosphor particles has occurred. After counting the total energy of all photons released in the cell as the heat, the heat source density $Q(\mathbf{r}, T)$ is obtained as the ratio of the energy to the cell volume.

6.2.3 Light absorption in the lamp units and optical boundaries

Heat in the lamp might also be released due to the light absorption in the lamp units and at the optical boundaries. The decrease in the photon intensity due to the light absorption in the lamp units follows Eq. (2.1). As a result, the heat source power in a certain grid cell in which the absorption occurs is defined as

$$Q_{abs} = W_{ph} [1 - \exp(-\alpha_i L_i)] \quad , \quad (6.7)$$



where α_i is the absorption coefficient of the cell and L_i is the length of the photon path inside that cell. The value of Q_{abs} is taken into account in the further heat transfer computations in a way similar to that described in Sec. 6.2.2.

As it was described in Sec. 2, the propagating photon with the energy W_{ph} might also be absorbed on the mirror-like or LED boundary, and this process is followed by the heat release at that boundary, which results in a surface heat flux q_s and is taken into account as a boundary condition (6.4).

7 References

- [1] M. Born and E. Wolf, "Principles of Optics: Electromagnetic Theory of Propagation, Interference and Diffraction of Light", Cambridge University Press (Cambridge) **1** (1999).
- [2] H.C. van de Hulst, "Light Scattering by Small Particles", John Willy & Sons, Inc (New York) **9** (1957).
- [3] H.C. van de Hulst, "Light Scattering by Small Particles", John Willy & Sons, Inc (New York) **7** (1957).
- [4] D. A. G. Bruggeman, "Berechnung verschiedener physikalischer Konstanten von heterogenen Substanzen", Ann. Phys. (Leipzig) **24** (1935) 636.
- [5] J. Monecke, "Bergman spectral representation of a simple expression for the dielectric response of a symmetric two-component composite", J. Phys.: Cond. Mat. **6** (1994) 907.
- [6] L. Henyey and J. Greenstein, "Diffuse radiation in the galaxy", Astrophys. J. **93** (1941) 70-83.
- [7] CIE (1995), Method of Measuring and Specifying Colour Rendering Properties of Light Sources, Publication 13.3, Vienna: Commission Internationale de l'Eclairage, ISBN 978-3900734572 (A verbatim re-publication of the 1974, second edition. Accompanying disk D008: Computer Program to Calculate CRIs)